involved in these processes could serve as models for charge separation in artificial photosynthetic systems.

Acknowledgment. This work was supported by the Consiglio Nazionale delle Ricerche (Comitato Chimica and Progetto Finalizzato Chimica Fine e Secondaria, Tematica Ah1).

Registry No. [2,2], 94499-30-6; [2,2,2], 94499-29-3; $[3,2]\cdot(PF_6)_3$, 94499-27-1; [3,2,2], 94499-28-2; $[3,2,3]\cdot(PF_6)_6$, 94499-25-9; $Ru(bpy)_2(CN)_2$, 58356-63-1; $[Ru(NH_3)_5Cl]Cl_2$, 18532-87-1.

The Iron(III) Complex of *N*-[2-((*o*-Hydroxyphenyl)glycino)ethyl]salicylidenimine. A Model Complex for the Iron(III) Environment in the Transferrins

Carl J. Carrano,*[1] K. Spartalian,[2] G. V. N. Appa Rao,[3] Vincent L. Pecoraro,[3,4] and M. Sundaralingam[3]

Contribution from the Department of Chemistry and the Department of Physics, University of Vermont, Burlington, Vermont 05405, and the Department of Biochemistry, University of Wisconsin, Madison, Wisconsin 53706. *Received June 1, 1984*

Abstract: The structure of an iron(III) complex of the *N*-[2-((*o*-hydroxyphenyl)glycino)ethyl]salicylidenimine (EHGS) has been determined by single-crystal X-ray diffraction. The complex crystallizes in the rhombohedral space group $R\bar{3}$ with a = 14.112 (2) Å, α = 107.49 (1)°. The metal ion is bound by the two nitrogen atoms, the two phenolate oxygen atoms, the carboxylate oxygen atom, and the oxygen atom of a coordinated methanol so as to describe a pseudooctahedral geometry about the metal. The nitrogens and the two phenolate oxygens form the equatorial plane with the metal lying on it. In aqueous solution the methanol is replaced by water. Optical titration shows that this coordinated water undergoes hydrolysis with a pK_a of 6.7. The hydrolysis has been followed by Mössbauer spectroscopy, and the aquo and hydroxo forms show distinct spectral signatures. These complexes serve as model compounds for the iron binding site in the transferrins as indicated by the similarity of their optical and magnetic parameters to those of the proteins. A novel interpretation of the iron binding site of the proteins is suggested.

The transferrins, also known as siderophilins, are vertebrate glycoproteins of about 80 000 daltons which tightly but reversibly bind 2 mol of ferric ion.[5-7] In mammals, serum transferrin is responsible for iron transport from sites of absorption to sites of storage and utilization and may have several other significant roles including "buffering" metal concentrations in the blood and acting as an antibacterial agent. The other members of the group, conalbumin, or ovotransferrin (egg white), and lactoferrin (milk and other mammalian secretions), do not have well-defined roles but may serve as antibacterials for their respective fluids. Despite their differing biological functions, all the siderophilins are known to contain very similar iron binding sites. Although the area of transferrin chemistry has been studied extensively, important questions remain on the nature and number of ligating groups that comprise the metal binding sites. Recent studies have focused on these questions by examining suitable small molecule model compounds whose stability constants and physical properties are similar to those of transferrin.[8-10] Our initial model was based on *N*,*N*'-ethylenebis[(*o*-hydroxyphenyl)glycine], EHPG. This ligand forms very stable complexes with Fe(III) and other transition elements by octahedrally encapsulating the metal ion, using two secondary amine nitrogen atoms, two carboxylate oxygen atoms, and two phenolate oxygen atoms. This assignment has been confirmed by X-ray structure determinations.[11,12] It is believed that the binding sites of transferrin contain two histidines,[13] two tyrosines,[8,14] a (bi)carbonate[15,16] anion, and water[17] or hydroxide[8] as a sixth ligand. EHPG has similar donor groups, but in one coordination position a carboxylate oxygen replaces a water molecule. For this reason we attempted to improve our model by synthesizing the pentadentate ligand *N*-[2-((*o*-hydroxyphenyl)glycino)ethyl]salicylidenimine, EHGS, which would allow a solvent molecule to occupy the sixth coordination site. Thus, the present complex more closely resembles the en-

(1) University of Vermont, Department of Chemistry.
(2) University of Vermont, Department of Physics.
(3) University of Wisconsin, Department of Biochemistry.
(4) Present address: Department of Chemistry, University of Michigan, Ann Arbor, MI 48109.
(5) Chasteen, N. D. *Coord. Chem. Rev.* **1977**, *22*, 1.
(6) Aisen, P.; Listowsky, I. *Annu. Rev. Biochem.* **1980**, *49*, 357.
(7) Chasteen, N. D. In "Advances in Inorganic Biochemistry"; Thiel, E. C., Eichorn, G. L., Marzilli, L. G., Eds.; Elsevier: New York, 1983.
(8) Pecoraro, V. L.; Harris, W. R.; Carrano, C. J.; Raymond, K. *Biochemistry* **1981**, *20*, 7033.
(9) Patch, M. G.; Simolo, K. P.; Carrano, C. J. *Inorg. Chem.* **1982**, *21*, 2972.
(10) Patch, M. G.; Simolo, K. P.; Carrano, C. J.; *Inorg. Chem.* **1983**, *22*, 2630.
(11) Pecoraro, V. L.; Riley, P. E.; Carrano, C. J.; Raymond, K. N.; *Inorg. Chem.* **1983**, *22*, 3096.
(12) Bailey, N. A.; Cummins, D.; McKenzie, E. D.; Worthington, J. M. *Inorg. Chim. Acta* **1981**, *50*, 111.
(13) Alsaadi, B. M.; Williams, R. J. P.; Woodworth, R. C. *Inorg. Biochem.* **1981**, *15*, 1.
(14) Tan, A. T.; Woodworth, R. C. *Biochemistry* **1969**, *8*, 3711.
(15) Zweier, J. L.; Woofen, J. B.; Cohen, J. S. *Biochemistry* **1981**, *20*, 3505.
(16) Que, L.; Schneider, D. J.; Roe, A. L.; Mayer, R. "Abstracts of Papers", 186th National Meeting of the American Chemical Society, Washington, DC, Aug 28-Sept 2, 1983; American Chemical Society: Washington, DC, 1983; INOR 156.
(17) Koenig, S. H.; Schillinger, W. E. *J. Biol. Chem.* **1969**, *244*, 6520.

0002-7863/85/1507-1651$01.50/0

Table I. Crystallographic Summary[a]

mol formula	$C_{19}H_{25}N_2O_6Fe$
M_r	433.27
$a = b = c$, Å	15.112 (2)
$\alpha = \beta = \gamma$, deg	107.49 (1)
V, Å^3	2833.96 (9)
cryst system	rhombohedral
space group	$R\bar{3}$ (C_{3i}^2, No. 148)
Z	6
d(calcd), g cm^{-3}	1.523
F(000)	1362
abs coeff, μ(Cu Kα), cm^{-1}	6.89
2θ interval, deg	3–50
crystal dimensions, mm^3	0.28 × 0.05 × 0.04
no. of reflcns measd	2725
no. of reflcns $I > 3\sigma(I)$	870
R	0.075
R_w	0.090

[a] Unit cell parameters were obtained by least-squares refinement of the setting angles of 15 reflections, in the range $21° < 2\theta < 46°$. Numbers in parentheses are the estimated standard deviations in the least significant digits.

vironmment implicated in the metal binding sites in the transferrins. In this work we interpret results from optical, electron paramagnetic resonance, and Mössbauer spectroscopy in correlation with the X-ray structure and establish the usefulness of the complex as a model for the transferrins. New interpretations of the binding sites in the proteins are suggested.

Materials and Methods

Materials. The ligand starting material, EHPG, was purchased from Sigma Chemical Co. and purified by Soxhlet extraction with acetone. All materials were reagent grade or better and used without further purification. Purity of the product was assayed via TLC on silica gel G-60 (Merck) precoated glass plates, using the upper layer of 1-butanol/H_2O/acetic acid (4:5:1) or pure methanol as eluant.

Preparation of Compounds. The title complex was prepared by a metal exchange between VO(EHGS) and $FeCl_3$ in methanol. The VO(EHGS) was prepared by a novel metal-assisted ligand decarboxylation of VO(EHPG) as previously reported.[18] The crude complex was purified by chromatography on neutral alumina (Sigma) using methanol as eluant. A blue band of the oxidized vanadium complex elutes first followed by a red band of the desired product. The product was crystallized from hot methanol to yield fine red needles, R_f 0.21 (silica gel/methanol eluant). These red needles were not suitable for X-ray diffraction as isolated. They analyzed as the aquo adduct of Fe(EHGS). Small quantities of dark brown rectangular crystals, suitable for X-ray diffraction, were grown from methanol after several crops of needles were removed. The X-ray structure shows that this material is the methanol solvate and not an aquo complex. Thus, the change in crystal habit can be attributed to substitution of water by methanol in the sixth coordination position. Early crops of the needle-like crystals (aquo complex) probably removed residual water from the methanol used for recrystallization. All solution data reported here are on the aquo complex as originally isolated. Both aquo and methanol adducts, however, yield the same species in solution as seen by their identical R_f values on TLC and identical optical and magnetic properties.

Anal. Calcd for Fe(EHGS)H_2O: C, 50.6; H, 4.7; N, 7.0. Found: C, 50.6; H, 4.1; N, 7.2.

X-ray Crystallography. The crystallographic data are given in Table I. X-ray intensity data for $2\theta < 50°$ were measured on an Enraf-Nonius CAD-4 diffractometer controlled by a DEC PDP-8/m computer, using Ni filtered Cu Kα radiation. Since the crystal diffracted weakly, out of a total of 2725 independent reflections collected, only 870 reflections had $I > 2\sigma(I)$, and these were used in the structure analysis. Lorentz, polarization, and crystal decay (ca. 15%) corrections were applied. No gross extinction was observed for any strong low-angle reflections at the end of structure refinement.

The structure was solved by using conventional Patterson and Fourier techniques and refined by block-diagonal least-squares methods. All non-H atoms of the complex including a methanol (solvent) molecule that is participating in the coordination polyhedron gave satisfactory refinement with anisotropic thermal parameters. The difference electron density map showed an additional methanol of solvation with the oxygen atom on the 3-fold axis and the methyl carbon 3-fold disordered. Both were given occupancy 0.333. The methanol molecule was therefore refined isotropically. The thermal parameters of this methanol are appreciably larger than the methanol participating in the coordination polyhedron. All hydrogen atoms except those on the disordered methanol were located in the difference Fourier maps, and they were fixed at these positions, with isotropic thermal parameters 4.0 Å^2. The final difference Fourier map was featureless. The final R value was 0.075 and R_w = 0.090. A modified Hugh's weighting scheme, $W = 1.0$ when $F_o < 34.0$ and $W = 34.0/F_o$ when $F_o > 34.0$, was applied. The scattering factors employed for the non-H atoms were taken from Cromer and Waber,[19] while those for H were taken from Stewart, Davidson, and Simpson.[20]

Spectral Titrations. Spectrophotometric titrations were performed in 25% methanol/water using 0.1 N NaOH as a titrant. Titrant was delivered by means of a Gilmont microburet and the pH recorded with an Orion 501 pH meter and combination electrode standardized at pH 4.0 and 10.0 with buffers (Fisher). The absorbance values at 490 nm vs. pH were fitted to a single ionization by using a modified version of a general nonlinear least-squares program, ORGLS.

Physical Measurements. Infrared spectra of samples in KBr pellets were obtained with a Nicolet 6000 FT-IR. Optical spectra were recorded on a Perkin-Elmer 552 spectrophotometer. Conductivity measurements were performed in methanol by using an Industrial Instrument RC16B2 bridge. The EPR data were obtained at 77 K with a quartz finger Dewar on a Varian E-4 spectrometer operating at 9.2 GHz. Samples were run in quartz tubes in a 5:1 (v/v) glycerine/water glass (or other solvents as indicated). DPPH or Fe(HEDTA) served as standards. Electrochemical measurements were performed in DMF (Burdick and Jackson) by using a platinum bead electrode and tetrabutylammonium hexafluorophosphate as a supporting electrolyte as previously described.[21] Magnetic moments were measured in solution by the Evans method and in the solid state with a Faraday balance of conventional design.

The Mössbauer spectrometer was of the constant acceleration type and was operated in connection with a 256 channel analyzer in the time scale mode. The source was ^{57}Co diffused in rhodium and was kept at room temperature at all times. Spectra were recorded in horizontal transmission geometry, and each run typically lasted 24 h. Calibrations were made by using the known hyperfine splittings in the metallic iron spectrum, and the isomer shifts reported here are relative to iron metal at room temperature. In calibrations with thin iron foils, line widths were typically 0.32 mm/s. An applied field of 0.13 T transverse to the γ beam was achieved with a permanent magnet. Samples were kept at 4.2 K by being immersed in liquid helium for the duration of the run. Lower temperatures were achieved by pumping on the liquid helium, and the temperature was determined from known vapor pressure–temperature data. Enriched samples were synthesized by using $^{57}FeCl_3$, prepared from 95% isotopically pure $^{57}Fe_2O_3$. Samples were dissolved in 5:1 glycerine/water and quick-frozen in liquid N_2.

Results

Synthesis and Characterization. The desired complex Fe(EHGS) was readily prepared by a transmetalation reaction between $FeCl_3$ and VO(EHGS) in methanol. The formulation as Fe(EHGS)H_2O, with water occupying the sixth axial coordination site, is supported by elemental analysis, infrared and optical spectroscopy, and analogy to the X-ray structure of the methanol complex (vide infra). The IR spectrum is extremely similar to the well-characterized VO(EHGS)[18] with C=N imine stretch at 1637 cm^{-1} but also with an OH stretch (from coordinated water) at 3436 cm^{-1}.

Conductivity measurements in methanol solution reveal the complex to be a nonelectrolyte, as expected from its formulation, indicating deprotonation and coordination by two phenolate and a carboxyl group along with the two nitrogens.

The presence of high-spin ferric ion in the complex was confirmed by magnetic susceptibility. At room temperature, a value of μ_{eff} = 5.8 (2) μ_B was found in solution and μ_{eff} = 6.0 (1) μ_B in the solid state, both near the spin-only value of 5.9 μ_B expected for high-spin ferric ion. This assignment is also supported by EPR and Mössbauer spectra.

Description of Structure. The asymmetric unit contains one Fe(EHGS) molecule in a general position. X-ray structure has

(18) Pecoraro, V. L.; Bonadies, J. A.; Marrese, C. A.; Carrano, C. J. *J. Am. Chem. Soc.* **1984**, *106*, 3360–3362.

(19) Cromer, D. T.; Waber, J. T. *Acta Crystallogr., Sect. B* **1965**, *B24*, 91.

(20) Stewart, R. F.; Davidson, E. R.; Simpson, W. T. *J. Chem. Phys.* **1965**, *42*, 3175.

(21) Marrese, C. A.; Carrano, C. J. *Inorg. Chem.* **1983**, *22*, 1958.

Table II. Fractional Positional Parameters for Non-Hydrogen Atoms (Values Are Multiplied by 10^4)

atom	x	y	z	B_{eq} or B
Fe	3473 (2)	276 (2)	7977 (2)	3.6 (1)
O1	3714 (8)	−905 (8)	7415 (8)	4.2 (5)
O2	3780 (9)	583 (9)	9360 (8)	5.0 (6)
O3	4907 (7)	1264 (8)	8243 (8)	4.0 (5)
O4	1963 (8)	−736 (9)	7408 (9)	5.7 (6)
O5	5935 (8)	1280 (9)	7451 (9)	5.6 (6)
O6[a]	1333 (60)	1333 (60)	1333 (60)	23.2 (6)
N1	3241 (10)	364 (10)	6521 (10)	4.5 (6)
N2	2977 (10)	1464 (10)	8139 (11)	4.3 (7)
C1	5109 (12)	1068 (12)	7455 (13)	4.1 (7)
C2	4125 (12)	346 (12)	6364 (12)	3.5 (7)
C3	4046 (11)	−714 (12)	6036 (12)	4.0 (7)
C4	4191 (12)	−1139 (13)	5165 (13)	5.0 (8)
C5	4156 (14)	−2158 (15)	4898 (15)	6.3 (10)
C6	3934 (16)	−2698 (14)	5416 (16)	6.8 (10)
C7	3775 (13)	−2281 (14)	6264 (15)	5.4 (9)
C8	3871 (13)	−1248 (13)	6615 (11)	4.1 (8)
C9	3101 (14)	1359 (14)	6587 (12)	4.7 (9)
C10	2517 (15)	1538 (14)	7177 (14)	5.9 (10)
C11	3166 (13)	2189 (13)	9012 (13)	4.9 (8)
C12	3542 (14)	2090 (14)	9938 (13)	5.4 (9)
C13	3663 (17)	2937 (17)	10829 (17)	8.1 (13)
C14	3986 (20)	2899 (21)	11804 (16)	8.4 (15)
C15	4161 (17)	2164 (18)	11941 (17)	8.0 (13)
C16	4119 (13)	1355 (16)	11097 (13)	5.7 (9)
C17	3801 (12)	1348 (14)	10124 (13)	4.4 (9)
C18	1223 (19)	−695 (20)	7736 (20)	10.4 (16)
C19[a]	1232 (59)	608 (63)	242 (61)	13.7 (50)

[a] These atoms were refined isotropically with a multiplicity of 0.33.

Table III. Selected Bond Angles (deg)

O(1)–Fe–O(2)	107.8 (7)	O(3)–Fe–N(1)	76.2 (7)
O(1)–Fe–O(3)	91.6 (7)	O(3)–Fe–N(2)	91.0 (8)
O(1)–Fe–O(4)	86.7 (7)	O(4)–Fe–N(1)	92.0 (7)
O(1)–Fe–N(1)	85.8 (7)	O(4)–Fe–N(2)	87.5 (8)
O(1)–Fe–N(2)	163.4 (7)	N(1)–Fe–N(2)	78.9 (8)
O(2)–Fe–O(3)	95.7 (7)	Fe–N(1)–C(2)	105.7 (13)
O(2)–Fe–O(4)	96.0 (7)	Fe–N(1)–C(9)	108.6 (13)
O(2)–Fe–N(1)	164.5 (8)	Fe–N(2)–C(11)	126.2 (15)
O(2)–Fe–N(2)	88.2 (8)	C(10)–N(2)–C(11)	119.1 (20)
O(3)–Fe–O(4)	168.2 (6)		

established that the solvent molecule occupying the sixth coordinating position is methanol, rather than a methoxide ion, as shown in Figure 1. Fractional positional parameters of the non-hydrogen atoms are given in Table II. Selected bond angles and bond lengths are in Tables III–IV. The ligand uses the two nitrogen and the two phenolic oxygen atoms to form the equatorial plane with the Fe atom only 0.017 Å out of this plane. The oxygen atoms from the carboxylate group and the methanol occupy the axial positions. The coordination polyhedron is that of a distorted octahedron. The bond lengths and angles in the coordination polyhedron are similar to the values found in other metal complexes of EHPG and EHGS.[12,18] Mean bond lengths in the coordination polyhedron are Fe–N 2.146 (15) Å, Fe–O(phenolic) 1.898 (12) Å, and Fe–O(trans) 2.058 (13) Å and are similar to the values found in Fe(EHPG)$^-$ complexes.[12] The variation in the cis bond angles at the coordinated metal ions of these complexes (EHPG, EHGS) of 75° to 109° and 79° to 108°, respectively, reflects a departure from more regular octahedral geometry. Most likely, this is a consequence of (a) the strain resulting from the coordination of a hexadentate vs. pentadentate ligand and (b) the requirement of planarity of the imine nitrogen atom of EHGS vis-à-vis the tetrahedral nitrogen atoms in EHPG.

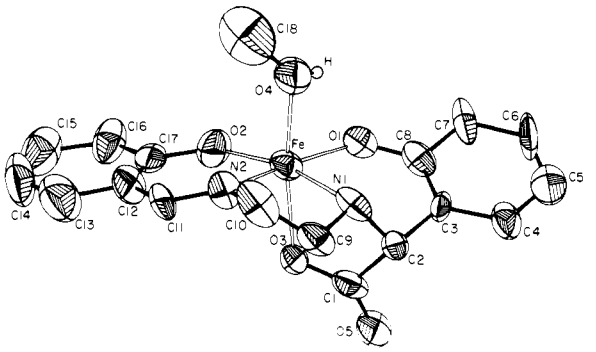

Figure 1. ORTEP drawing, showing the molecular structure and atom labeling scheme in the [Fe(EHGS)·CH_3OH] complex.

The torsion angles in the main chain of the ligand in the present and related complexes[12,18] are given in Table V. The torsion angles are nearly equal in the Fe and V complexes of EHGS. The torsion angles in the Mg salt of racemic Fe(EHPG)$^-$ show a pseudo-2-fold symmetry around C9–C10 that cannot occur with Fe(EHGS) because of the oxidation of the N2–C11 bond. The main differences between EHGS and EHPG are in the torsions around the C1–N2 and C11–C12 bonds.

Table IV. Comparison of the Bond Lengths (Å) in the Coordination Polyhedron of the Related Complexes

complex	$M-O_1$	$M-O_2$	$M-O_2$	$M-O_4$	$M-N_1$	$M-N_2$	displacement of M from equatorial plane
Fe(EHGS)·CH_3OH[a]	1.925 (13)	1.872 (11)	2.063 (12)	2.053 (14)	2.173 (14)	2.121 (16)	0.017
Na(VO(EHGS))	1.950	1.943	2.281	1.609	2.126	2.055	0.377
$Mg(Fe(EHPG))_2$	1.904 (3)	1.918 (3)	2.047 (2)	2.037 (3)	2.157 (3)	2.175 (3)	0.007
Na(Fe(EHPG))							
molecule 1	1.922 (7)	1.893 (7)	2.011 (8)	2.087 (8)	2.157 (8)	2.140 (9)	0.699
molecule 2	1.904 (8)		2.029 (8)		2.151 (9)		0.0

[a] The bond lengths for the imine bond N(2)–C(11) and the amine bond N(1)–C(2) are 1.32 (2) and 1.43 (3) Å, respectively.

Table V. Torsion Angles (deg) of the Related Complexes in the Main Chain of the Ligands

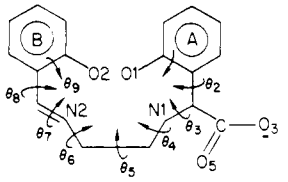

complex name	θ_1	θ_2	θ_3	θ_4	θ_5	θ_6	θ_7	θ_8	θ_9
Fe(EHGS)·CH_3OH	3.8	−53.1	−164.9	−154.8	49.6	132.0	175.5	2.7	4.7
Na(VO(EHGS))	−1.7	−57.2	−169.7	−148.0	47.2	136.0	−179.7	0.2	1.3
$Mg(Fe(EHPG))_2$	−4.1	−40.3	−169.4	−154.5	56.2	−157.1	−165.3	−53.3	−3.6
Na(Fe(EHPG))									
molecule 1	1.4	−47.6	−168.5	−158.5	59.7				
molecule 2	2.9	−50.3	−166.1	−149.6	54.2	−167.4	47.7	46.3	−1.9

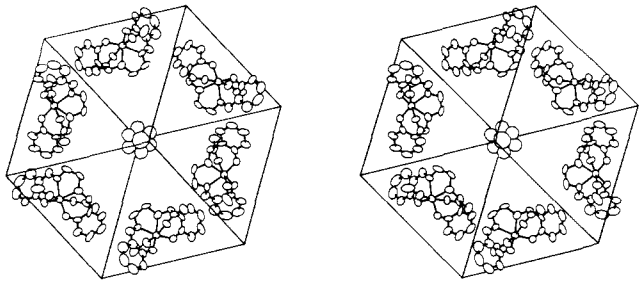

Figure 2. Stereoview of the unit cell down the 3-fold axis. Notice the disordered methanol of solvate on the 3-fold axis.

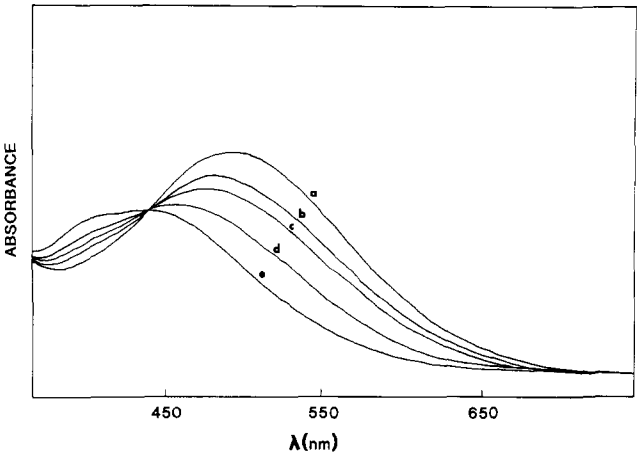

Figure 3. Optical absorption spectrum of Fe(EHGS) in 25% MeOH/H_2O as a function of pH: (a) 4.9; (b) 6.2; (c) 6.5; (d) 7.0; (e) 7.8.

An interesting feature of the present structure is the packing of the molecules in the cell. Figure 2 shows the packing down the 3-fold axis. There is a large void around the 3-fold axis, which is occupied by the methanol of solvation. The closest atom to this methanol in the unit cell is C18, which is 3.69 (10) Å away. Therefore, this methanol is free to rotate around the 3-fold axis, resulting in the high thermal vibration of the molecule. Some evaporation of the methanol from the crystal probably accounts for the crystal "decay" (15%) observed during X-ray irradiation. The only major intermolecular interaction other than van der Waals interaction between the molecules is the hydrogen bond between the coordinated methanol hydroxyl proton and the carboxylate oxygen (O4···O5, 2.60 (2) Å).

Optical Spectra. The optical spectrum of Fe(EHGS) is essentially identical in methanol or 25% methanol/water and displays an intense transition at 497 nm, ϵ_m = 4024 L/(mol cm). This transition has been assigned, by analogy to numerous similar complexes, as being a L → M charge transfer from a pπ orbital on the phenolate oxygen to the half-filled metal t_{2g} orbital.[22,23] A second weaker transition is observed as a shoulder at 420 nm. This second band could be due to a ligand-based π–π^* transition of the imine that is considerably shifted. The analogous band appears at 360 nm in the vanadyl complex. Alternatively it may arise from a second LMCT to an e_g metal orbital. The energy difference, 3000 cm^{-1}, between the two transitions would then be a measure of $10D_q$ in a strictly octahedral complex. This value is much too low, however ($10D_q$ is expected to be ca. 10000 cm^{-1}), and the symmetry of the complex is clearly less than octahedral. Thus, the difference probably measures the splitting of the t_{2g} orbitals due to the lowered symmetry.

The addition of base to a solution of Fe(EHGS) in methanol/water results in spectral changes over the pH range from 4 to 9 such as those seen in Figure 3. The color is observed to change from dark red to yellow-orange with the maintenance of an isosbestic point at 440 nm, indicating a simple two-species equilibrium. This equilibrium involves a single deprotonation of the coordinated water molecule.

$$Fe(EHGS)H_2O \overset{K}{\rightleftharpoons} Fe(EHGS)OH^- + H^+$$

The spectrophotometric analysis of such a process has been described.[24] By use of the appropriate equations, the data could be fitted well (Figure 4) and refined to give values of log $K_{MH_{-1}L}$ = 6.74 and $\epsilon_{MH_{-1}L}$ 2088 L/(mol cm). This represents the pK_a of the coordinated water and is at least 4 log units lower than the hydrolysis observed for the corresponding coordinatively saturated EHPG complexes. Thus, the open coordination site yields hydrolytic products at lower pH values as expected. The pK_a of the water ligand is in the range observed for other complexes of iron that contain coordinated water.[25,26]

As might be expected for a complex with an open coordination site, the optical spectra show a pronounced solvent dependence. While red solutions are observed in the solvents methanol and water, paler orange solutions are seen in the donor solvents, pyridine, Me_2SO, DMF, and methylimidazole. Spectral data are tabulated in Table VI and show blue-shifted spectra in these solvents with generally lower extinction coefficients. The spectra and visible color of Fe(EHGS) solutions in donor solvents resemble those of the deprotonated complex in water or methanol. Qualitatively similar blue shifts were seen upon dissolving Fe(EHPG)$^-$ complexes in good donor solvents.[9]

Electrochemistry. The hydrolysis of the coordinated water is also reflected in the electrochemical behavior of these complexes as determined by cyclic voltammetry. In methanol, a single quasi-reversible (peak to peak separation, 86 mV, $i_{pc}/i_{pa} \simeq 1$), one-electron reduction is observed. The potential of this process is −509 mV vs. SCE. The addition of base (tetraethylammonium hydroxide) to the red solution causes color changes similar to those previously described. A new wave grows in at ca. −620 mV while the original couple shifts negatively and decreases in intensity.

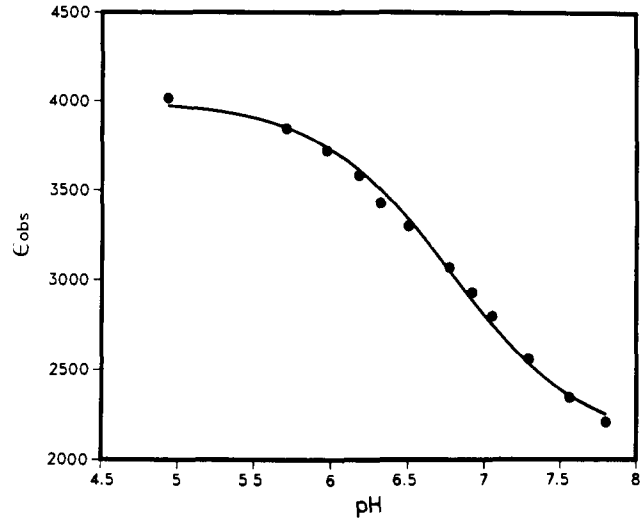

Figure 4. Absorbance vs. pH for the titration of Fe(EHGS). The solid line is a computer fit to a single ionization with pK = 6.74.

Table VI. Optical Spectral Parameters for Fe(EHGS) in Various Solvents

solvent	λ_{max}, nm	ϵ, L/(mol cm)
methanol	497	4024
pyridine	490	1830
methyl imidazole	480	
Me_2SO	475	2334
DMF	475	3921

(22) Patch, M. G.; Carrano, C. J. *Inorg. Chim. Acta* **1981**, *56*, L71.
(23) Gaber, B. P.; Miskowski, V.; Spiro, T. G. *J. Am. Chem. Soc.* **1974**, *96*, 6868.
(24) Harris, W. R.; Carrano, C. J.; Raymond, K. N. *J. Am. Chem. Soc.* **1979**, *101*, 2722.
(25) Branca, M.; Checconi, P.; Pispisa, B. *J. Chem. Soc., Dalton Trans.* **1976**, 481.
(26) Branca, M.; Pispisa, B.; Aurisicchio, C. *J. Chem. Soc., Dalton Trans.* **1976**, 1543.

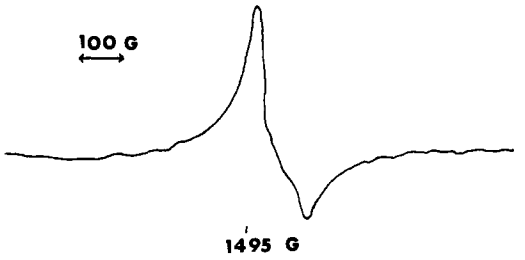

Figure 5. EPR spectrum of Fe(EHGS), "pH" 4.9, at 77 K in a 5:1 glycerine/water glass.

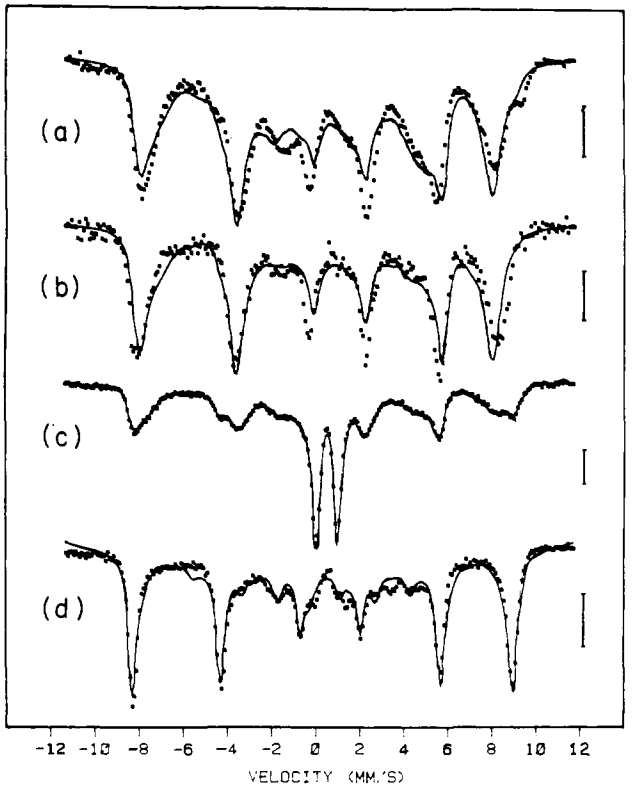

Figure 6. Mössbauer spectra of frozen Fe(EHGS) in an applied field of 130 mT. (a) T = 4.2 K, pH 4.9; (b) T = 1.5 K, pH 4.9; (c) T = 4.2 K, pH 7.2; (d) T = 4.2 K, pH 9.2. The solid lines are computer simulations as explained in the text. Bars indicate 1% absorption.

Eventually, the initial wave is gone and the new couple predominates. Deprotonation of the coordinated water leads to a negatively charged hydroxo complex that is harder to reduce than the aquo complex.

EPR. The EPR spectrum of Fe(EHGS) in a "pH" 4[27] 5:1 glycerine/water glass at 77 K shows features clustered around g = 4.3, indicative of high-spin Fe(III) in a rhombic electronic environment. Peaks are seen at 149.0 and 159.5 mT with a saddle point at 152.5 mT (Figure 5). As the "pH" is raised, the spectrum begins to collapse until at "pH" 11 it is nearly isotropic (peaks at 150.2 and 154.5 mT), indicating a more rhombic environment. Obvious changes are observed in polar donor solvents as well. The spectra in DMF, pyridine, or phenol look similar and are characterized by a sharp central feature and broad shoulders with an overall width of 25 mT. By comparison Fe(EHGS) in glycerine/water glass shows a spectral width of about 8 mT.

Mössbauer Spectroscopy. Figure 6 shows Mössbauer spectra of frozen Fe(EHGS) solutions in 5:1 glycerine/water at 4.2 K. An external magnetic field of 130 mT was applied perpendicular to the γ-beam direction. We note a marked dependence of the spectral profile on the pH value: The low-pH Mössbauer spectrum in Figure 6a shows paramagnetic hyperfine structure with relatively broad but clearly defined absorption lines. The shoulder at about 9.2 mm/s is attributed to the second excited Kramers doublet and indicates that the zero field splitting parameter, D, is relatively small. The spectrum in Figure 6b taken at 1.5 K shows a clean six-line pattern as the contributions from the excited Kramers doublets are reduced in intensity by thermal depopulation. The neutral pH spectrum (Figure 6c) shows three species of iron, one that is fast relaxing, as seen by the narrow peaks at the center of the spectrum, and two that are slow relaxing with a magnetic hyperfine field typical of high-spin ferric ion. The slow relaxing spectrum is a mixture of two: the spectrum at low pH and the one at high pH. The high-pH spectrum (Figure 6d) shows only one species of iron. Comparison of the spectra at high and low pH shows that the former has significantly narrower absorption lines, larger zero field splittings, and a slightly larger magnetic hyperfine field at the nucleus. There is no evidence of the fast relaxing component at pH 4.9 or 9.8. In analogy to the methanol found in the X-ray structure, we assign a water molecule to the sixth ligand position at low pH. At high pH this water molecule becomes deprotonated, forming a hydroxo complex in agreement with the spectral titration results. At intermediate pH we have the coexistence of the aquo and hydroxo species as well as a site that shows fast electronic relaxation.

In order to investigate the reproducibility of these results, Mössbauer spectra of a sample were recorded at increasing pH values to a maximum of pH 10. Then spectra were recorded as the pH was lowered to the same values. The spectra were reproducible to within our ability to determine the pH of a 5:1 glycerine/water solution. In particular we noticed that the fast relaxing component appears only around neutral pH values and is not present at low or high pH.

The Mössbauer spectra at high and low pH were fitted by computer using the method of least-squares to a spin Hamiltonian with $S = {}^5/_2$ that includes quartic terms:

$$\mathcal{H} = D[S_z^2 - S(S+1)/3 + \lambda(S_x^2 - S_y^2) + (\mu/6) \times (S_x^4 + S_y^4 + S_z^4)]$$

The spin Hamiltonian parameters that provide the best fits (solid lines in Figure 6a,b,d) are shown in Table VII. The solid line in Figure 6c is not a fit but a composite of (a) 56% of the spectrum at pH 4.9 (Figure 6a), (b) 23% of the spectrum at pH 9.8 (Figure 6d), and (c) 21% of a quadrupole doublet with isomer shift δ = 0.52 mm/s, quadrupole splitting ΔE = 0.95 mm/s, and line width Γ = 0.36 mm/s.

The spectrum from the hydroxo complex at high pH can be fitted well with a D value that is relatively large. This indicates that the middle and upper Kramers doublets, associated with the ground electronic sextet, are not significantly populated at 4.2 K, and the details of the spectrum can be reproduced with a quadratic-only spin Hamiltonian. The spin Hamiltonian parameters of this complex are in line with similar complexes[28-30] except for the value of the quadrupole splitting, which is somewhat low by comparison.

Table VII. Mössbauer and Spin Hamiltonian Parameters for Fe(EHGS)

	low pH (aquo)	high pH (hydroxo)
isomer shift, δ mm/s[a]	0.54	0.50
quadrupole splitting, ΔE, mm/s[b]	1.60	0.42
asymmetry parameter, η	0.35	0.93
line width, Γ, mm/s	0.53	0.39
magnetic coupling, $A/g^*_n\beta_n$, T	20.7	22.1
zero-field splitting, D, cm^{-1}	0.16	1.72
rhombic parameter, λ	0.97	0.34
quartic parameter, μ	−1.45	0.0

[a] With respect to metallic Fe. [b] $\Delta E = (V_{zz}/2)(1 + \eta^2/3)^{1/2}$; $V_{zz} > 0$ in both cases.

(27) Meter reading in 5:1 glycerine/H_2O.

(28) Spartalian, K.; Oosterhuis, W. T.; Neilands, J. B. *J. Chem. Phys.* **1975**, *62*, 3538.
(29) Lang, G.; Assa, R.; Garbett, K.; Williams, R. J. P. *J. Chem. Phys.* **1971**, *55*, 4539.
(30) Spartalian, K.; Carrano, C. J. *J. Chem. Phys.* **1983**, *78*, 4811.

In the aquo complex at low pH, the spin Hamiltonian parameter λ is not between 0 and $^1/_3$, Blumberg's[31] conventional range of values. We note that it is not always possible to adhere to this convention if one correlates EPR and Mössbauer results, especially when the contributions from *all three* Kramers doublets are seen in the Mössbauer spectra. In the quadratic spin Hamiltonian formulation, the $g = 4.3$ signal requires $\lambda = {}^1/_3$, and this forces the three Kramers doublets to be equally spaced in energy by 3.5 D. Thus, the quadratic-only spin Hamiltonian does not have enough flexibility to provide for a $g = 4.3$ signal when the three Kramers doublets happen not to be equally spaced in energy. Initial trial fits to the low pH complex showed that a quadratic-only spin Hamiltonian with $\lambda \simeq {}^1/_3$ provides unacceptably poor simulations of the Mössbauer spectra. If D were made small enough to reproduce the shoulder at 9.2 mm/s, which is associated with the upper doublet, the middle doublet's contribution in the simulation was more significant than observed. It is possible, however, to increase the separation between the bottom and middle doublets (thus decreasing the latter's contribution to the spectrum) and at the same time preserve the separation between the bottom and upper doublets without sacrificing the $g = 4.3$ signal by considering quartic terms in the spin Hamiltonian. Quartic parameter μ subject to the "isotropy condition" $\mu = 0.75(1-3\lambda)$ reproduces the $g = 4.3$ signal over the entire range of λ values.[28]

With the inclusion of quartic parameter μ, the "best" fit to the Mössbauer spectrum at low pH became acceptable but not impressive (Figure 6a). A much better fit, with the same parameters, was obtained for the sample at 1.5 K (Figure 6b), indicating that this spin Hamiltonian formulation does not fully account for the contributions from the middle and upper doublets. Because the 1.5 K spectrum is associated almost entirely with the bottom Kramers doublet, we place more confidence in the values for the quadrupole splitting, ΔE, and the magnetic hyperfine field H_{int} than in the spin Hamiltonian parameters λ and μ. It is likely that a single set of spin Hamiltonian parameters is inapprorpiate for the low-pH complex. The broad lines indicate a distribution of magnetic hyperfine field values at the nucleus presumably because of slight variations in the crystal field environment at the iron sites, which in turn may suggest a distribution of D, λ, and μ values. This has been observed in the Mossbauer spectra of hexaaquoiron,[32] another complex with low D values.

Discussion

The present model, $Fe(EHGS)H_2O$, possesses many of the chemical and physical characteristics of the iron binding site of the transferrins as measured by optical, EPR, and Mössbauer spectroscopy. The model provides two nitrogen, two phenolate, and a carboxylate donor group from the chelate backbone and leaves open a single coordination site where either water or hydroxide are seen to bind. We will now compare the results of our physical measurements on Fe(EHGS) with those from the transferrins.

The optical spectra of transferrins show a characteristic charge-transfer transition at about 465 nm ($\epsilon_M \simeq 2500$/Fe) that is responsible for their salmon pink color. The aquo form of Fe(EHGS) has a similar transition that is red-shifted to 495 nm. The related complexes *meso*-, and *rac*-$Fe(EHPG)^-$ have respective bands at 485 and 475 nm.[10] The red shift of Fe(EHGS) with respect to Fe(EHPG) is not surprising because the negative charge in the latter will tend to push the CT band to higher energy. While aquo Fe(EHGS) is distinctly red with an extinction coefficient that is higher ($\epsilon_M \simeq 4000$/Fe) than that of transferrin, conversion to the hydroxo form results in a yellow complex with a band of reduced intensity ($\epsilon_M \simeq 3000$/Fe) that is shifted to $\lambda_{max} = 440$ nm. At neutral pH $\lambda_{max} = 465$ nm and the color is remarkably close to transferrin. Thus, from the viewpoint of optical spectroscopy, the greatest similarity occurs when there is an average between the aquo and hydroxo forms.

The optical spectra of Fe(EHGS) are solvent dependent. In solvents such as *N*-methylimidazole, pyridine, DMF, or Me_2SO the spectra are blue-shifted with transitions of generally reduced intensity. The solvent effects could arise from simple displacement of water by solvent in the axial coordination site. We do not believe that this is the case, however, because *N*-methylimidazole, a nitrogen donor, and DMF and Me_2SO, oxygen donors, give similar optical and EPR spectra.[33] Furthermore, similar spectral shifts are seen with the coordinatively saturated Fe(EHPG) complexes in these same solvents.[10] We believe that the spectral changes are probably caused by bonding between high donor number solvents such as DMF, Me_2SO, and pyridine and the coordinated water. Such an interaction would lead to a lengthening of one of the O–H bonds and a shortening of the Fe–O bond (see Gutman's rules, ref 34). This would lead to a net decreasing positive charge on the iron and a shift in a LMCT to higher energy as observed. The similarity to the deprotonated complex is thus a matter of degree of O–H bond lengthening, with the extreme being complete loss to yield a hydroxo complex.

The interpretation of the EPR results from serum transferrin[35] in terms of a spin Hamiltonian gives $D = 0.31$ cm^{-1}. The interpretation of the Mössbauer results[36-38] gives D values in the range 0.15–0.25 cm^{-1}. The disagreement between the two techniques is not as important as is the general agreement that transferrin has a relatively low D value, lower than other $g = 4.3$ complexes.[39] In a previous study[30] we sought the interpretation of the electronic structure of the $g = 4.3$ complexes in terms of a crystal-field model. It was possible to construct a crystal-field model that successfully accounted for the EPR, Mössbauer, and optical spectra of the Fe(EDTAH). We found that the same model may be used as the basis of a crystal-field interpretation for the EPR and Mössbauer spectra of several $g = 4.3$ complexes provided that their zero-field splittings correspond to D values larger than about 0.6 cm^{-1}. Although we have not yet applied the crystal-field formulation to the electronic structure of $g = 4.3$ complexes with low D values, it is apparent that these complexes belong in a category by themselves.

Even though we do not have an exact match of the electronic structure at the iron site, we place aquo Fe(EHGS) in this same category. To our knowledge, aquo Fe(EHGS) is the first transferrin model complex with zero-field splittings that are remarkably close to those of the proteins. We recognize that the EPR spectrum of aquo Fe(EHGS) does not reproduce the "double horn" feature that is characteristic of the EPR spectra from the transferrins, but failure to reproduce this feature does not indicate overall failure of the model. The EPR spectra are particularly sensitive to the spin Hamiltonian parameters λ and μ; these are not identical, nor are they expected to be so, for aquo Fe(EHGS) and transferrin. We further note that a match of the spin Hamiltonian parameters may not necessarily mean a match of the EPR spectra. Attempts to simulate the EPR spectra of serum transferrin by using a spin Hamiltonian with quadratic and quartic terms met with no success.[40] This may indicate inherent shortcomings in the spin Hamiltonian formulation or, more likely, the presence of at least two separate iron environments, each with its own electronic structure.

We interpret the Fe(EHGS) spectrum at neutral pH as having contributions from three separate species of iron. Two of these are the aquo and hydroxo sites. The third species gives rise to

(31) Blumberg, W. In "Magnetic Resonance in Biological Systems"; Ehrenberg, A., Malmstrom, B. G., Vanngard, T., Eds.; Pergamon Press: Oxford, 1967.
(32) Knudsen, J. E. *J. Phys. Colloq.* (*Orsay, Fr.*) **1976**, 735.
(33) Pyridine as a solvent may be an exception since its spectrum is not substantially blue-shifted and shows a pronounced peak at 425 nm where the other solvents show only a shoulder; nevertheless, the EPR spectra of Fe(EHGS) in pyridine and in DMF are alike.
(34) Gutman, V.; Resch, G.; Linert, W. *Coord. Chem. Rev.* **1982**, *43*, 133.
(35) Pinkowitz, A.; Aisen, P. *J. Biol. Chem.* **1972**, *247*, 7830.
(36) Spartalian, K.; Oosterhuis, W. T. *J. Chem. Phys.* **1973**, *59*, 617.
(37) Tsang, C. P.; Boyle, A. J. F.; Morgan, E. H. *Biochim. Biophys. Acta* **1973**, *328*, 84.
(38) Tsang, C. P.; Bogner, L.; Boyle, A. J. F. *J. Chem. Phys.* **1976**, *65*, 4584.
(39) Oosterhuis, W. T. *Struct. Bonding* (*Berlin*) **1974**, *20*, 59.
(40) Scullane, M. I.; White, L. K.; Chasteen, N. D. *J. Magn. Reson.* **1982**, *47*, 383.

the quadrupole pair at the center of the spectrum and indicates a magnetic hyperfine field at the nucleus that is time averaged to zero. We propose that the quadrupole pair indicates the formation of a dimer, bridged at the sixth coordination site. A plausible scheme requires the existence of a hydrogen oxide bridge of the type recently reported[41,42] for some trinuclear cluster ions. The bridge is formed by a strong hydrogen bond between a hydroxide ligand on one complex with an aquo ligand on another. Bino and Gibson have proposed that bridges of this type should be pH dependent.[41] At low pH, Fe(EHGS) is entirely in the aquo form; at higher pH, near the pK_a, the aquo and hydroxo forms coexist and may form hydrogen oxide bridged dimers;

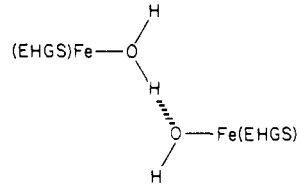

at even higher pH (pH > pK_a), only the hydroxo form exists and the dimer disappears. This pattern is predicted by the model of Bino and Gibson, who have proposed that the $H_3O_2^-$ bridge may be a general feature in the hydrolysis of mononuclear metal ions such as $Fe(H_2O)_6^{3+}$. Our results seem to support this view.

This bridging model may provide a mechanism for the fast relaxing sites seen only at neutral pH (Figure 6c). As the bridging proton is shared between the two atoms, it is possible that each iron site in the dimer fluctuates between the aquo and hydroxo states. Rapid relaxation between the two states would cause the magnetic hyperfine field at the nucleus to average to zero because the aquo and hydroxo states are not expected to have hyperfine fields that are identical in magnitude and direction. Furthermore, in the fast relaxation regime, the quadrupole splitting is expected to have a value that is obtained by averaging the components of the EFG between the two states. The resulting value for the quadrupole splitting would depend on the relative orientation between the EFG axes; however, the values of 1.6 and 0.4 mm/s are far enough apart to ensure that the averaged quadrupole splitting falls between these two values. A spin–spin relaxation process is unlikely because it usually gives rise to poorly defined hyperfine structure with broad-winged absorption lines and because it cannot account for the appearance of the fast relaxing component at pH near the pK_a having a quadrupole splitting that is neither aquo- nor hydroxo-like.

In transferrins, the occupancy of the sixth coordination site has been a subject of controversy, with either water or hydroxide as the likely candidates. Our study of the two forms of Fe(EHGS) does not point to a clear-cut choice of one or the other for all the proteins in the group but suggests instead that both may be important and in fact linked to the question of whether the obligate anion is carbonate or bicarbonate. We believe that the electronic structure of aquo Fe(EHGS) is similar enough to those of the transferrins to consider the possibility of water as the sixth ligand in the coordination sphere of iron. If indeed this is the case, we have to explain the proton stoichiometry. It is known[43] that three protons are released upon iron binding in the transferrins, and these have been attributed to the deprotonation of three tyrosine residues[43] or two tyrosines and a coordinated water.[8] We find the independent evidence for two tyrosine coordination compelling, but if the third proton does not come from a coordinated water molecule, we have to seek its source.

The nature of the bound anion as carbonate or bicarbonate is related to the proton release since a single proton would be given up if the anion binds as carbonate and none if it binds as bicarbonate. Several studies designed to address this question have reported conflicting conclusions. The recent study by Zweier et al.[15] using ^{13}C NMR seems to provide reasons for the confusion.

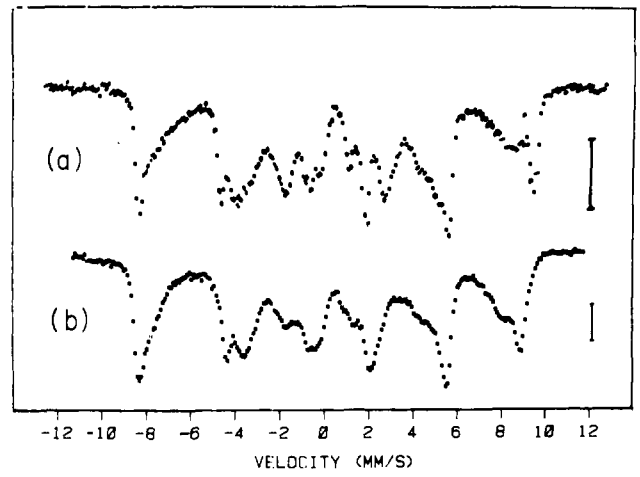

Figure 7. (a) Mössbauer spectrum of diferric ovotransferrin at 4.2 K in a small transverse field, same as Figure 5d in ref 45. (b) Artificial Mössbauer spectrum generated by adding 60% of the spectrum in Figure 5a (low pH) and 40% of the spectrum in Figure 5d (high pH). Bars indicate 1% absorption.

It appears that there are a multiplicity of forms of the bound anion that may depend on the specific protein, bound metal ion, pH, extraneous ions, etc. Thus, when cobalt is bound to serum transferrin, carbonate may be the anion at one of the two metal sites in the protein and bicarbonate at the other. In his recent review[7] Chasteen suggested that, strictly speaking, it may be inappropriate to distinguish between carbonate and bicarbonate as the form of the bound anion. The nature of the anion may simply be a matter of degree, with the two extreme forms being carbonate and bicarbonate. We concur with this view and link it to the question of whether the nature of the water bound to the iron is aquo or hydroxo.

It is now established that the anion is bound to the protein through a positively charged group, viz. histidine, arginine, or lysine or perhaps a combination of these, and is also bound directly to the iron in the ternary complex. Thus, if we model the binding site as shown below, we can explain the proton stoichiometry.

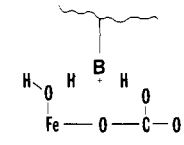

The extent to which the protons belong to particular groups depends on the relative base strengths in the ternary complex. These could be perturbed by a number of factors including the nature of bound metal, conformational differences between specific proteins, or changes caused by external anions such as perchlorate, etc. The two extreme cases are obviously aquo and carbonate or hydroxo and bicarbonate, with various intermediate cases possible. Charge relay schemes of the kind described here are known in several enzymes such as serum proteases,[44] alcohol dehydrogenase, etc.

The consideration that both aquo and hydroxo forms may coexist, perhaps in the same protein, suggested a reexamination of the Mössbauer spectra[45] of diferric ovotransferrin (OTF) for which no spin Hamiltonian formulation has been reported. If we choose to view the OTF Mössbauer spectrum as the sum of two components, one with lines that are narrower than the other, we note the following: (a) The narrow component in OTF has peaks at the same positions as hydroxo Fe(EHGS); (b) the broad component in OTF shows a magnetic hyperfine field that is smaller than the narrow component and occurs at approximately the same positions as aquo Fe(EHGS). We added the spectra from aquo

(41) Bino, A.; Gibson, D. *Inorg. Chem.* **1984**, *23*, 109.
(42) Bino, A.; Gibson, D. *J. Am. Chem. Soc.* **1982**, *104*, 4383.
(43) Gelb, M. H.; Harris, D. C. *Arch. Biochem. Biophys.* **1980**, *200*, 93.
(44) Blow, D.; Birktoft, J. J.; Hartley, B. S. *Nature (London)* **1970**, *221*, 337.
(45) Aisen, P.; Lang, G.; Woodworth, R. C. *J. Biol. Chem.* **19738** *248*, 649.

and hydroxo Fe(EHGS) in a 60:40 mixture and obtained the spectrum in Figure 7b. Spectrum 7a is from Fe(OTF) and is identical with spectrum 4d in ref 45. The 60:40 mixture was chosen to match the peaks at −4 mm/s. Comparison between the spectra in Figure 7 shows similarities and differences. The composite Fe(EHGS) spectrum reproduces fairly well the OTF peaks outside the region ±2 mm/s. The central region is not reproduced as faithfully, but we do not reasonably expect to match all the features in the OTF spectrum. After all, simple addition of the EPR spectra from aquo and hydroxo Fe(EHGS) does not yield a composite that resembles the OTF EPR spectrum. Differences in and between Fe(EHGS) and OTF are expected to give rise to differences in the EPR spectra and to a mismatch between central regions in the Mössbauer spectra where the middle doublet contribution is most prominent. Nevertheless, our results seem to support a possibility suggested in ref 45, namely that both OTF iron sites exist in more than one conformation, resulting in different ligand fields and, hence, in different spin Hamiltonian parameters. On the basis of our present study of Fe(EHGS), we find it reasonable to identify these conformations in OTF with one that favors an aquo-like configuration at the iron and one that favors a hydroxo-like configuration.

The relative weight of each environment in the binding site will be governed by the conformations of the protein chain. Chaotropic agents such as perchlorate and thiocyanate have been known to perturb the native conformation/conformations by binding to several specific sites remote from the iron.[46] The EPR[47] and Mössbauer[48] spectra of transferrins reflect these perturbations, which indicates transmission of information to the iron sites. The model we propose for the binding site in these proteins provides a simple way of perturbing the iron environment by altering the proton relay so as to favor either a hydroxo or an aquo environment.

(46) Folastar, D. A.; Chasteen, N. D. *J. Am. Chem. Soc.* **1982**, *104*, 5775.
(47) Price, E. M.; Gibson, J. F. *J. Biol. Chem.* **1972**, *247*, 8031.
(48) Lang, G., unpublished results.

Summary

We present a crystallographic determination of a novel Fe(III) complex with an open coordination site where solvent can bind. In aqueous solution the coordinated water can undergo hydrolysis at near neutral pH to yield a hydroxo complex. Interpretation of magnetic measurements on these complexes suggests that they may serve as models of the iron binding sites in the transferrins. Study of the models indicates that the nature of the sixth ligand (aquo/hydroxo) in the proteins is linked by a proton relay mechanism to the form of the obligate anion (carbonate/bicarbonate). We substantiate a previous suggestion[45] that two conformations of the iron binding site may coexist in ovotransferrin. The two conformations are distinguished by the presence of a water molecule or hydroxide as the sixth ligand of the iron. Extension of this model to other iron tyrosinate proteins is in progress.

Acknowledgment. Work at the University of Vermont was supported by Research Corporation grants to C.J.C. and K.S., for which we are grateful. We thank J. A. Bonadies and C. T. Bailey for their excellent technical assistance. Crystallographic work at the University of Wisconsin was partially supported by NIH Grant GM-17378 and by the College of Agricultural and Life Sciences, University of Wisconsin. A government of Indian fellowship to G.V.N.A.R. and an NIH postdoctoral fellowship to V.L.P. are gratefully acknowledged. We thank Prof. K. N. Raymond and Dr. P. Riley for prepublication release of the X-ray data on Na[VO(EHGS)].

Registry No. Fe(EHGS)H_2O, 90432-10-3; VO(EHGS), 89890-28-8; Fe(EHGS)MeOH, 94706-21-5.

Alkyne-Induced Carbyne–Carbyne Coupling in the Trinuclear Bis(carbyne) Iron Cluster $Fe_3(CO)_9(\mu_3\text{-}COC_2H_5)(\mu_3\text{-}CCH_3)$. X-ray Structures of $Fe_3(CO)_6(\mu\text{-}CO)_2\text{-}\mu_3\text{-}\eta^4[C(OC_2H_5)C(CH_3)C(C_6H_5)C(C_6H_5)]$ and $Fe_3(CO)_6(\mu\text{-}CO)_2\text{-}\mu_3\text{-}\eta^4[C(CH_3)C(OC_2H_5)C(Si(CH_3)_3)C(Si(CH_3)_3)]$

Didier Nuel, Françoise Dahan, and René Mathieu*

Contribution from the Laboratoire de Chimie de Coordination du CNRS associé à l'Université Paul Sabatier, 31400 Toulouse, France. *Received July 18, 1984*

Abstract: The reaction of alkynes R_1CCR_2 with the trinuclear bis(carbyne) iron cluster $Fe_3(CO)_9(\mu_3\text{-}COC_2H_5)(\mu_3\text{-}CCH_3)$ produces complexes in which coupling of the entering alkynes with the carbyne ligands has occurred. X-ray structure determinations of the resulting $Fe_3(CO)_6(\mu\text{-}CO)_2(R_1CCR_2)(C(OC_2H_5)C(CH_3))$ complexes in the cases where $R_1 = R_2 = C_6H_5$ or $Si(CH_3)_3$ show the presence of $Fe\text{–}C(C_6H_5)\text{–}C(C_6H_5)\text{–}C(CH_3)\text{–}C\text{–}(OC_2H_5)$ and $Fe\text{–}C(Si(CH_3)_3)\text{–}C(Si(CH_3)_3)\text{–}C(OC_2H_5)\text{–}C(CH_3)$ ferracyclopentadiene rings. Extension to other alkynes like acetylene and phenylacetylene or *tert*-butylacetylene revealed a third situation in which the ferracyclopentadiene rings result from the insertion of the alkynes between the two carbyne ligands. Spectroscopic data also suggest that in the case of phenyl- and *tert*-butylacetylene, the ferracyclopentadiene ring results from the carbon–carbon breaking of alkynes and coupling of the resulting carbyne fragments. Mechanisms for these observations are proposed and discussed.

The proposal that molecular metal clusters may be reasonable models for the interactions of organic molecules with metal surfaces[1] has induced in the past few years numerous works on the reactions between clusters and unsaturated organic molecules.[2] The problem of chain growth in the Fischer–Tropsch reaction is specifically at the origin of numerous studies on the chemistry of polynuclear alkylidene complexes.[3] However, the field of the

(1) Muetterties, E. L.; Rhodin, N. T.; Band, E.; Brucker, C. F.; Pretzer, W. R. *Chem. Rev.* **1979**, *79*, 91–137.

(2) Deeming, A. J. In "Transition Metal Clusters"; Johnson, B. F. G., Ed.; Wiley: New York, 1980; pp 391–469.

0002-7863/85/1507-1658$01.50/0